IEEE Access
Multidisciplinary ⋮ Rapid Review ⋮ Open Access Journal

Received June 4, 2022, accepted June 14, 2022, date of publication June 20, 2022, date of current version June 23, 2022.

Digital Object Identifier 10.1109/ACCESS.2022.3184320

Optimization of Injection-Compression Molding Processing Conditions for Fresnel Lens Based on Optical Performance and Geometry Deformation Considerations

CHAO-MING LIN AND TING-HSUAN MIAU
Department of Mechanical and Energy Engineering, National Chiayi University, Chiayi 600355, Taiwan
Corresponding author: Chao-Ming Lin (cmlin@mail.ncyu.edu.tw)

This work was supported by the Ministry of Science and Technology of Taiwan under Grant MOST 109-2221-E-415-001-MY3, Grant MOST 109-2221-E-415-002-MY3, and Grant MOST 108-2813-C-415-007-E.

ABSTRACT Mold flow simulations are performed to determine the processing conditions which optimize the optical performance and geometry deformation of a plastic Fresnel lens manufactured using the injection-compression molding (ICM) technique. Due to the quality requirements of plastic optical components in ICM manufacturing (it is hoped to achieve the goals of minimum deformation and minimum birefringence), and pursuing the above two conflicting objectives and meeting the quality requirements at the same time is the best product optimization. The analysis process is to optimize optical path difference and optical axial displacement individually by Taguchi method, and two sets of processing parameters are obtained respectively. Based on these data, a set of processing parameters that can optimize two objectives at the same time is obtained by using the grey relational analysis. If the above process cannot obtain optimal result, the fixed factor method can fix the most significant factor and continue to process the optimization analysis of the remaining factors. The results show that the presented method can indeed solve the problems of dual-objectives optimization and large differences in the influence of factors.

INDEX TERMS Fixed-factor, Fresnel lens, grey relational analysis, injection-compression molding, optical axial displacement, optical path difference, Taguchi method.

I. INTRODUCTION

Injection compression molding (ICM) is one of the most commonly used methods for the manufacturing of plastic optical components. As shown in Fig. 1a, in the ICM process, the mold is left partially open with a compression gap during the filling stage. Compression gap is a processing factor for injection compression molding, which is the distance between two molds before the nozzle injects a certain amount of melt into the cavity through the runner. This spacing is used to make the stroke that the mold will move during the subsequent clamping process. However, once the pre-set volume of melt has been injected into the cavity, the mold is clamped (Fig. 1b); thereby producing a uniform compression force throughout the cavity. The packing and cooling stages of the molding cycle are then performed as usual (Fig. 1c). Finally, the mold is opened, and the finished component (e.g., a Fresnel lens) is ejected (Fig. 1d) [1]–[4]. Compared to the traditional injection molding process, ICM reduces the injection pressure required to fill the cavity and improves the uniformity of the compression force within the mold. As a result, it reduces the residual stress within the final component, and hence improves the imaging quality by minimizing the birefringence and optical aberrations [5]–[8]. However, the melt flow process of plastic molding is highly complex, and involves the interaction between many non-linear, non-stable, and time- or temperature-dependent properties [9], [10]. Hence, determining the optimal processing parameters for the ICM process using an experimental trial-and-error approach is extremely time-consuming and expensive. By contrast, mold flow analyses provide a cost-effective solution for exploring the behavior of polymer melt within even the most complex of molds through a process of numerical simulation. Compared to traditional experimental

The associate editor coordinating the review of this manuscript and approving it for publication was Jingang Jiang.

This work is licensed under a Creative Commons Attribution 4.0 License. For more information, see https://creativecommons.org/licenses/by/4.0/

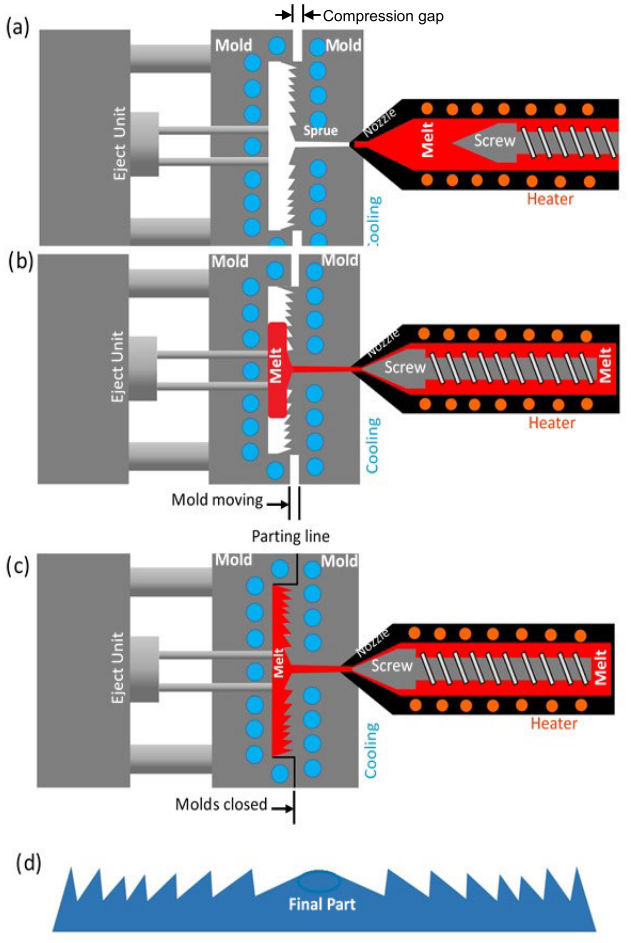

FIGURE 1. Schematic illustration of injection-compression molding (ICM) process. (a) Initial compression gap reserved in mold cavity before injecting melt. (b) Melt injected into enlarged cavity. (c) Melt compressed by mold movement. (d) Final part (Fresnel lens) ejected from mold.

techniques, mold flow analysis methods provide a far cheaper and more systematic approach for exploring the effects of the mold design and processing conditions on the characteristics of the final part. Consequently, computer aided engineering (CAE) software, such as Moldex3D, Moldflow, Inspire Mold, ANSYS, Deform3D are widely used throughout the plastic and metal manufacturing industry optimization analysis. [11]–[14]. Fresnel lenses replace the curved surface of conventional convex lenses with a series of concentric grooves (see Figs. 2a and 2b). They are thus thinner and lighter than their conventional counterparts, but retain a similar (if not better) focusing and light collection performance.

As a result, they are used in many applications nowadays, including automobile headlamps, solar collection systems, overhead projectors, hand-held magnifiers, and so on [15]–[17]. As with many other optical components, Fresnel lenses are generally produced using the ICM process. However, the circular wave geometry of the lens poses significant challenges to the molding process, and an appropriate design of the processing parameters is thus essential in ensuring

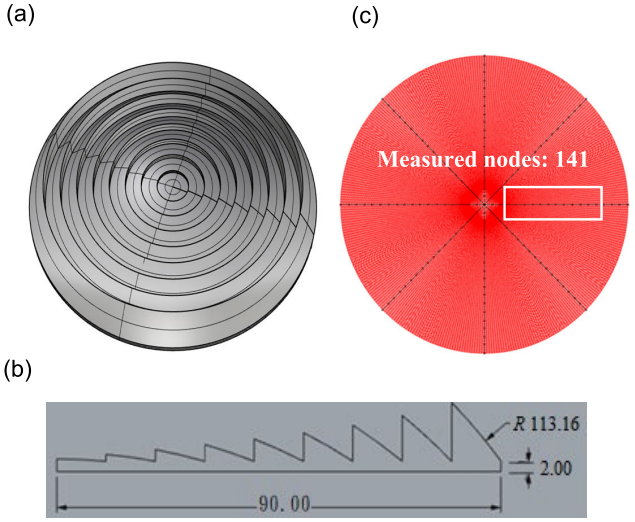

FIGURE 2. Fresnel lens. (a) Geometry model. (b) Cross-sectional dimensions of half-Fresnel lens (units: mm). (c) Numerical mesh and measurement nodes. (Mesh nodes:1086054; Mesh elements: 1098120; Measured nodes: 141).

the quality of the final part. In practice, it is desirable to minimize both the birefringence properties of the lens and the aberrations. Thus, in optimizing the molding process, it is necessary to determine the processing conditions which minimize the optical path difference (OPD) through the lens (caused by residual stress) and the optical axis displacement (OAD) (caused by warpage deformation) [18], [19].

In general, for the optimization of a single target (either OPD or OAD), Taguchi method should be able to obtain excellent results after proper selection of factors and levels. However, for simultaneous optimization for two goals, Taguchi method combined with gray relation theory can also obtain good results in the similar quality tendency. But, if Taguchi-GRA method is aimed at two goals with conflicting qualities (for example: OAD and OPD in this study), it is necessary to properly classify and deal with special impact factors. Thus, in the present study, a simulation approach based on Moldex3D mold flow analysis software [20] is used to determine the optimal settings of the ICM processing conditions which minimize the OPD and OAD of a molded plastic Fresnel lens. The simulations consider three main optimization methods, including the Taguchi analysis method, grey relational analysis (GRA), and a fixed-factor (FF) Taguchi analysis method, where these methods are used either alone, or in conjunction with one another [21], [22].

II. MANUFACTURING QUALITY AND OPTICAL PERFORMANCE OF ICM-PRODUCED OPTICAL LENSES

For the manufacturing quality of optical lenses, the main defect formation is due to surviving processing stresses after demolding. During injection compression molding, molded parts often have non-uniform cooling rates due to local

differences in part thickness, geometric design, material properties, etc. As a result, the part exhibits uneven surviving processing stress, leading to warpage in the final product. On the other hand, a certain amount of stress (residual stress) inevitably remains in the part and freezes in the part as it cools, causing birefringence.

A. STRESSES AFFECTING MANUFACTURING QUALITY

Injection-molded plastic components undergo significant thermal loads, mechanical loads, and phase change during the molding cycle, and thus inevitably contain a certain degree of surviving stress following cooling and removal from the mold. Broadly speaking, the all processing induced stress can be categorized as either flow induced stress or thermal induced stress. Flow induced stress arises since the polymer chains within the melt tend to align in a direction relative to the flow direction during the filling stage of the molding cycle, and have insufficient time to relax and return to their original configurations during the packing and cooling stages. Meanwhile, thermally induced stress is caused by rapid cooling rates (i.e., high temperature gradients) during molding, resulting in uneven volumetric shrinkage of plastic parts, or warping of parts after they are released from the mold. In this paper, the stress contained in the final molded product is called residual stress. Such residual stresses can affect optical performance and are discussed further in the following section.

B. BIREFRINGENCE

For an optical lens, the presence of residual stress causes a change in the local refractive index, which induces an optical path difference through the lens and leads to birefringence [23]–[25]. In particular, for incident light consisting of two orthogonally-polarized light waves, the light is split into two components (referred to as the o-ray (ordinary ray) and e-ray (extraordinary ray), respectively) at the incident boundary, which then take slightly different paths through the lens [26]. In practical applications, the degree of birefringence depends on the orientation of the molecules within the product, and is thus directly related to the magnitude of the residual stress. According to the stress-optic (Brewster's) law, the magnitude of the birefringence is given by [27]

$$n_1 - n_2 = C_B\,(\sigma_1 - \sigma_2), \tag{1}$$

where n_1, n_2 are the refractive indices along the principal axes, C_B is the relative stress-optic coefficient in Brewsters, and σ_1, σ_2 are the principal stresses.

C. OPTICAL PATH DIFFERENCE (OPD) AND OPTICAL AXIS DISPLACEMENT (OAD)

For an optical lens with birefringence, the optical path difference (OPD) or retardation is defined as the product of the distance traveled by the light in the lens and the refractive index difference for the two light rays. In other words, the OPD is proportional to the thickness of the lens, and is given mathematically as

$$\Delta_{12} = (n_1 - n_2)\,t = 2\pi C_B t\,(\sigma_1 - \sigma_2)\big/\lambda, \tag{2}$$

where Δ_{12} is the optical path difference (or retardation) and t is the lens thickness.

The number of fringes for the birefringence effect is then given by

$$N = \Delta_{12}/2\pi = C_B t\,(\sigma_1 - \sigma_2)\,/\lambda, \tag{3}$$

where N is the number of fringes and λ is the incident light wavelength.

Meanwhile, the optical axis displacement (OAD) is defined as the deformation (i.e., warpage) of the lens in the optical axis direction and is computed as the average position offset of all the calculation nodes of the analysis model relative to the optical axis direction before and after processing, respectively.

III. MOLD FLOW ANALYSIS AND OPTIMIZATION METHOD

The present study combines Moldex3D simulations with optimization theory to determine the ICM processing conditions which minimize the OPD and OAD of a plastic Fresnel lens. Fig. 3a shows the main steps in the proposed simulation framework. As shown, four optimization schemes are considered, namely: (I) single-objective Taguchi optimization of the OPD, (II) single-objective Taguchi optimization of the OAD, (III) multi-objective Taguchi-GRA optimization of the OPD and OAD, and (IV) multi-objective Taguchi-GRA-FF optimization of the OPD and OAD. The details of each of the main steps shown in Fig. 3a are described in the following. Fig. 3b shows the flow chart of ICM simulation including the CAD designing, the mold building, the boundary conditions setting, the processing factors setting, the solver analyzing, and the result analyzing.

A. GEOMETRY MODEL AND PLASTIC OPTICAL MATERIAL

The simulations considered the Fresnel lens shown in Figs. 2a and 2b with a radius of 90 mm, a curvature radius of 113.16 mm and a thickness of 2 mm. A 3D model of the lens was constructed in Rhinoceros and Moldex3D Mesh software with a total of 1086054 nodes and 1098120 elements. For each set of molding conditions, the lens was sectioned in the radial direction and the nodal displacement was measured at 141 measurement nodes, as shown in Fig. 2c. The model was then exported to Moldex3D mold flow analysis software to design the corresponding mold cavity, gate, runner and cooling system. In performing the simulations, the lens was assumed to be fabricated of ACRYREX®CM-205; a polymethyl methacrylate (PMMA) feedstock material produced by Chi-Mei Corporation (Taiwan) with the material properties shown in Table 1.

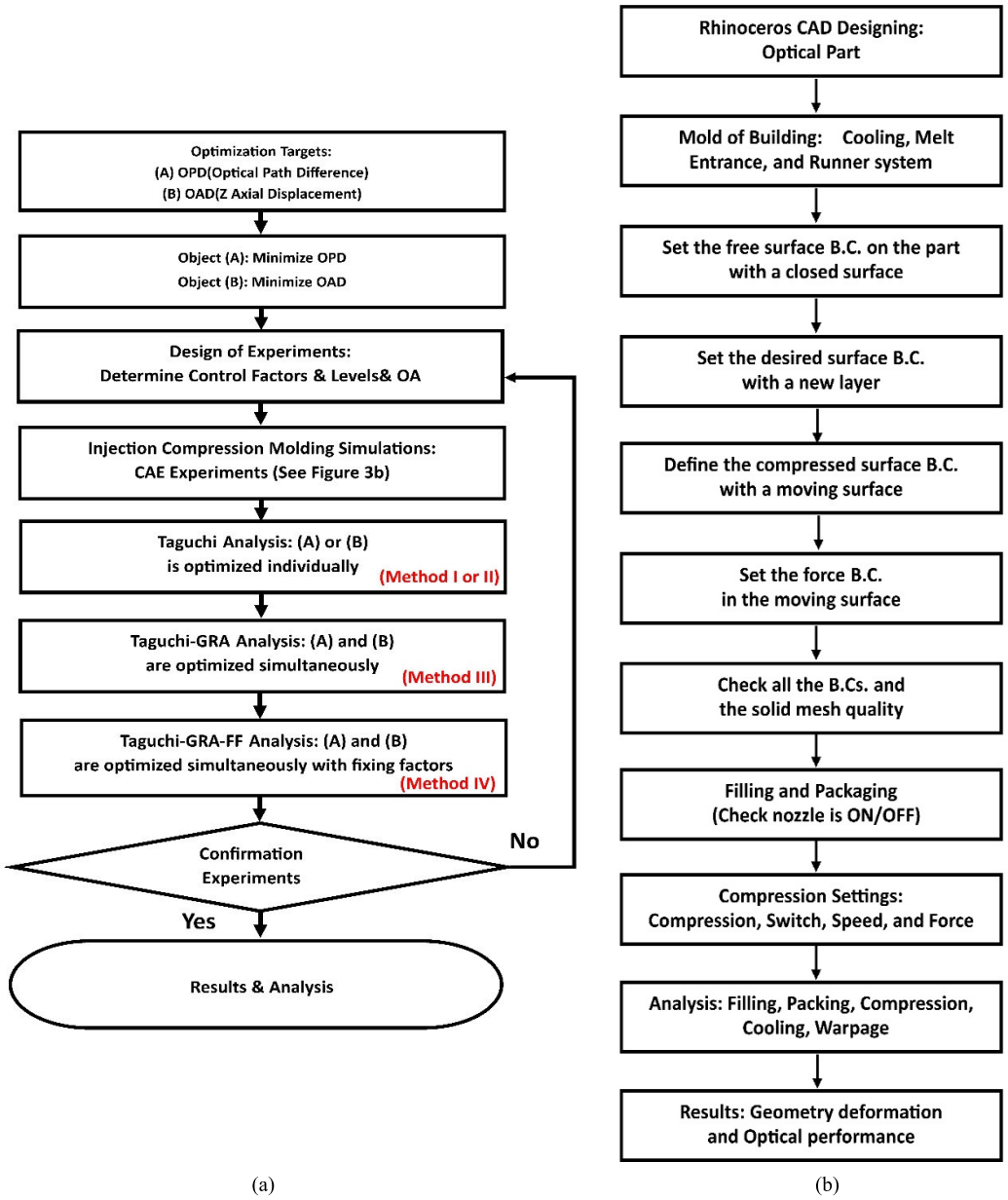

FIGURE 3. (a) Flow chart showing main steps in integrated Taguchi, Taguchi-GRA and Taguchi-GRA-FF Taguchi framework for optimization of OPD and OAD of Fresnel lens. (b) Flow chart of Injection Compression Molding Simulation.

B. TAGUCHI OPTIMIZATION METHOD (METHODS I AND II)

The OPD and OAD are taken as the quality characteristics of the lens, while the ideal function is smaller. The optimization experiments considered six control factors, namely (A) the filling time, (B) the melt temperature, (C) the mold temperature, (D) the compression gap, (E) the maximum compression speed, and (F) the cooling time. In the designation of experiment, specific Orthogonal Array (OA) is a type of general fractional factorial design. It is based on an orthogonal design matrix, and allows user to consider a selected subset of combinations of multiple factors at multiple levels. Orthogonal arrays are balanced to ensure that all levels of all factors are considered equally in statistics. Since many processing factors of the injection compression process must be considered, the OA-$L_{25}(5^6)$ with 6 factors is selected. As shown in Table 2, each control factor was assigned five level settings. Consequently, the Taguchi trials were configured in an $L_{25}(5^6)$ orthogonal array (OA), as shown in Table 3. Calculate the S/N value through the Taguchi experiment (larger is better), and convert it into a factor response graph. Among them, the maximum S/N value of each factor is the optimal level of the factor. After combining the factors, one can get the best control factor (processing parameters) for the

TABLE 1. Material properties of PMMA (ACRYREX® CM-205, CHIMEI).

Material Property	Data	Unit
Melt Flow Index	1.8	g/10 min
Mass Density	1.19	-
Bulk Density	0.7	g/cm^3
Water Absorption	0.3	%
Mold Shrinkage	0.2-0.6	%
Hardness	95	M scale
Light Transmission	92	%
Tensile Strength (Break)	750	Kg/cm^2
Tensile Elongation	10	%
Flexural Strength	1200	Kg/cm^2

TABLE 2. Control factors and level settings for Taguchi analysis (OPD and OAD).

Control factors	A (s)	B (°C)	C (°C)	D (mm)	E (mm/s)	F (s)
Level 1	1	210	50	2	10	5.2
Level 2	1.5	220	55	2.5	12.5	5.4
Level 3	1.8	230	60	3	15	5.6
Level 4	2	240	65	3.5	17.5	5.8
Level 5	2.5	250	70	4	20	6

target result. The aim of the simulation experiments was to determine the ICM processing conditions which minimized the OPD and OAD of the manufactured lens. Hence, the quality of each experimental outcome in the Taguchi OA for each objective criterion (OPD or OAD) was evaluated using the following formula:

$$R = -10\log\left(\bar{y}^2 + S_n^2\right), \tag{4}$$

$$S_n = \sqrt{\frac{\sum_{i=1}^{n}(y_i - \bar{y})^2}{n}}, \tag{5}$$

where R is the signal-to-noise ratio; $\mathbf{y_i}$ is the OPD, OAD, or grey relational grade (in the case of Methods III and IV); $\bar{y}$ is the average value of $\mathbf{y_i}$, and n is the number of measured points in each trial [28]–[31].

C. TAGUCHI-GRA OPTIMIZATION METHOD (METHOD III)

Methods I and II are single-objective optimization methods which yield the optimal processing conditions for either the OPD (Method I) or OAD (Method II). However, there is no guarantee that the optimal processing conditions for the OPD are the same as those for the OAD. Hence, in Method III, the S/N values obtained from the Taguchi experiments for the two different objective criteria are further analyzed by GRA in a two-objective optimization process designed to determine the processing conditions which jointly minimize both the OPD and the OAD. Grey relation analysis (GRA) is one of the most widely used models of Grey system theory, and

TABLE 3. Configuration of Taguchi experiments in $L_{25}(5^6)$ orthogonal array.

Trials	A	B	C	D	E	F	Trials	A	B	C	D	E	F
1	1	1	1	1	1	1	**14**	3	4	1	3	5	2
2	1	2	2	2	2	2	**15**	3	5	2	4	1	3
3	1	3	3	3	3	3	**16**	4	1	4	2	5	3
4	1	4	4	4	4	4	**17**	4	2	5	3	1	4
5	1	5	5	5	5	5	**18**	4	3	1	4	2	5
6	2	1	2	3	4	5	**19**	4	4	2	5	3	1
7	2	2	3	4	5	1	**20**	4	5	3	1	4	2
8	2	3	4	5	1	2	**21**	5	1	5	4	3	2
9	2	4	5	1	2	3	**22**	5	2	1	5	4	3
10	2	5	1	2	3	4	**23**	5	3	2	1	5	4
11	3	1	3	5	2	4	**24**	5	4	3	2	1	5
12	3	2	4	1	3	5	**25**	5	5	4	3	2	1
13	3	3	5	2	4	1							

the degree of relationship between sequences is characterized using a metric referred to as the grey relational grade; a positive number with a value less than or equal to 1, where a higher value indicates the presence of a greater relevance among the factors [32]–[36]. In the proposed method, the S/N values obtained from Eq. (4) for the two optimization criteria (i.e., the OPD and OAD) are first normalized to values in the interval of 0 to 1 using the formula.

$$x_i^* = \frac{x_i^{(0)}(k) - min\left\{x_i^{(0)}(k)\right\}}{max\left\{x_i^{(0)}(k)\right\} - min\left\{x_i^{(0)}(k)\right\}}, \tag{6}$$

where $min\left\{x_i^{(0)}(k)\right\}$ is the smallest value of $x_i^{(0)}(k)$; and $max\left\{x_i^{(0)}(k)\right\}$ is the largest value of $x_i^{(0)}(k)$.

Having computed the normalized sequences, the grey relational coefficient is calculated between each sequence and the reference sequence in accordance with

$$\Delta_{ij}(k) = \left\|x_i(k) - x_j(k)\right\|, \tag{7}$$

$$\gamma\left(x_i(k), x_j(k)\right) = \frac{\min\left\{\Delta_{ij}(k)\right\} + \xi\max\left\{\Delta_{ij}(k)\right\}}{\Delta_{ij}(k) + \xi\max\left\{\Delta_{ij}(k)\right\}}, \tag{8}$$

here $i = 1, 2, 3, \ldots, m; j = 1, 2, 3 \ldots, m; k = 1, 2, 3, \ldots, n$; $\Delta_{ij}(k)$ is the absolute value difference between $x_i(k)$ and $x_j(k)$; $x_i(k)$ is the reference series and $x_j(k)$ is the comparison series; $\gamma\left(x_i(k), x_j(k)\right)$ is the grey relational coefficient; $\min\left\{\Delta_{ij}(k)\right\}$ is the smallest value of $\Delta_{ij}(k)$; $\max\left\{\Delta_{ij}(k)\right\}$ is the largest value of $\Delta_{ij}(k)$, and ξ is a distinguishing coefficient with a value in the interval of $\xi \in [0, 1]$. The distinguishing coefficient is an important parameter of GRA. Scholars generally assume that $\xi = 0.5$, and good analysis results have also been obtained in the field of engineering

optimization. Some scholars believe that the change of ξ does not affect the ranking of factors through GRA [37], [38]. Some scholars think it will affect the analysis results that the distinguishing coefficient modifies the range of environmental conditions and further controls the relative difference between the gray correlation coefficients related to the problem [39]. Therefore, it can be inferred that ξ will change according to the uncertainty of the data [40]. The smaller the value of ξ, the greater the distinguishability between data sequences, the larger the value of ξ, the smaller the distinguishability. In this study, the distinguishing coefficient ξ is 0.5, which is in line with the set value of most engineering analysis. In general, the grey relational coefficient has a value in the range of 0 to 1, where a value of 0 indicates that the two sequences are completely unrelated, while a value of 1 indicates that the sequences are completely related. Having calculated the grey relational coefficients of all the competing alternatives, the grey relational grade of each alternative, i.e., $\Gamma\left(x_i, x_j\right)$, is evaluated as

$$\Gamma\left(x_i, x_j\right) = \frac{1}{n}\sum\nolimits_{k=1}^{n} \gamma\left(x_i\left(k\right), x_j\left(k\right)\right), \tag{9}$$

D. TAGUCHI-GRA-FF OPTIMIZATION METHOD (METHOD IV)

Since Method III is a multi-objective optimization process, which aims to jointly minimize both the OPD and the OAD, there is a risk that the solutions obtained for the two quality criteria may be sub-optimal compared to those obtained using the respective single-objective Taguchi analysis methods. Accordingly, in the final optimization method, the control factor having the greatest effect on the outcomes of the OPD and OAD criteria in the single-objective Taguchi experiments is identified and assigned its optimal value. The Taguchi-GRA optimization procedure (Method III) is then repeated using this fixed control factor level setting. To reduce extreme effects, this fixed control factor level is usually set at the midpoint of the levels that can cause two opposite effects. The resulting S/N values are then analyzed to determine the processing conditions which simultaneously optimize both the OPD and the OAD. For confirmation purposes, Method III is repeated once again using the optimal parameter settings for all of the processing parameters other than the fixed control factor, which is assigned each possible level setting in turn. Finally, the S/N ratios obtained in the confirmation experiment for different fixed control factor level settings are compared with those obtained in Methods I and II to confirm (or otherwise) the optimal setting of the fixed control factor level.

IV. RESULTS AND DISCUSSION

The innovative part of this research is mainly for the optimization analysis of the processing parameters of the injection compression molding process (ICM) for two conflicting quality goals (OPD and OAD), using (Method I, II) individual Taguchi method (to obtain the opposite optimization trend: You can choose a single optimization method depending on the target demand), using (Method III) Taguchi method combined with GRA (the optimized results cannot be obtained at the same time: you can get both optimized or partial optimization results depending on the target demand), and using (Method IV) Taguchi method combines GRA and FF (you can get the result of simultaneous optimization). Finally, the user can select an appropriate optimization method according to the needs of the optimization target to achieve the quality characteristics of the product. The main results are discussed below.

A. TAGUCHI OPTIMIZATION OF OPD AND OAD USING METHODS I AND II

Table 4 shows the S/N factor response results obtained from Method I for the OPD quality characteristic of the Fresnel lens. As shown in the bottom row of the table, the six control factors can be ranked in order of diminishing effect on the OPD as follows: melt temperature > compression gap > filling time > maximum compression speed > cooling time > mold temperature. Furthermore, observing the range values of each control factor, it is evident that the melt temperature (range=5.14777 dB) dominates the OPD outcome, while the other factors exert only relatively minor effects. Fig. 4a shows the S/N response diagram for the OPD quality characteristic. With the change of the melt temperature level value of the orthogonal table design, it also confirms that the melt temperature has the most significant influence when the OPD is the target. Considering the eighth trial as the standard processing conditions for the chosen ICM machine, the OPD effect of the optimized trial has been significantly improved, as shown in Fig. 4b. The aim of Method I is to determine the processing conditions which minimize the OPD of the molded lens. In other words, the objective of the optimization process is to establish the factor level settings which maximize the S/N ratio given in Eq. (4). Hence, the results presented in Fig. 4a indicate that the optimal processing conditions for the OPD characteristic are as follows: "(A5) filling time 2.5 s, (B5) melt temperature 250°C, (C5) mold temperature 70°C, (D5) compression gap 4 mm, (E1) maximum compression speed 10 mm/s, and (F1) cooling time 5.2 s. The results presented in Fig. 4b confirm that these optimal parameter settings improve the S/N ratio (i.e., reduce the OPD) compared to that of any of the other experimental trials in the Taguchi OA (including the standard processing conditions given in Row #8 of the OA). Table 5 shows the S/N factor response results obtained from Method II for the OAD. As shown, the control factors can be ranked in terms of a reducing effect on the OAD as follows: melt temperature > maximum compression speed > filling time > compression gap > mold temperature > cooling time. The OAD is once again determined mainly by the melt temperature. However, the effect of the melt temperature on the OAD is less intense than that on the OPD (i.e., S/N=7.67 dB vs. S/N=-50.899). Referring to Fig. 5a, it is inferred that the optimal processing conditions for minimizing the OAD are as follows: (A2) filling time 1.5 s, (B1) melt temperature 210°C, (C3) mold temperature 60°C, (D5) compression gap 4 mm,

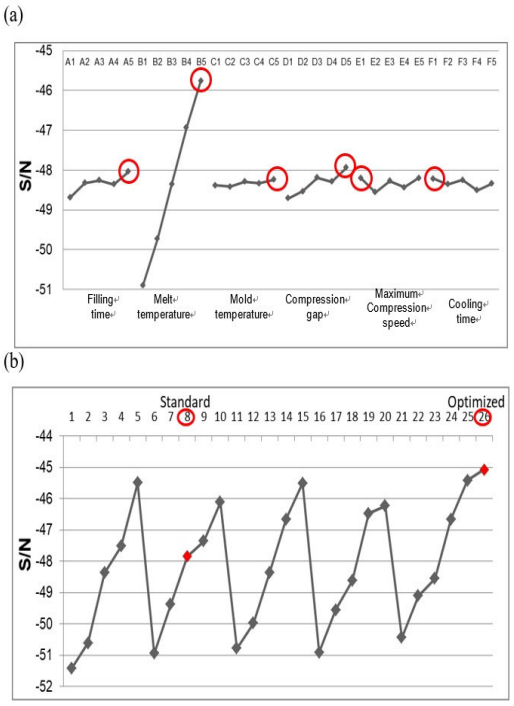

FIGURE 4. (a) Response diagram and (b) Confirmation results for optimization of OPD using method I.

TABLE 4. S/N response table for optimization of OPD using method I.

(dB)	A	B	C	D	E	F
Level 1	-48.685	-50.899	-48.384	-48.707	**-48.194**	**-48.213**
Level 2	-48.325	-49.726	-48.416	-48.534	-48.560	-48.354
Level 3	-48.257	-48.351	-48.286	-48.187	-48.274	-48.251
Level 4	-48.356	-46.933	-48.332	-48.294	-48.432	-48.505
Level 5	**-48.037**	**-45.751**	**-48.242**	**-47.94**	-48.2	-48.338
range	0.64766	5.14777	0.17450	0.76656	0.36619	0.29172
rank	3	1	6	2	4	5

TABLE 5. S/N response table for optimization of OAD using method II.

(dB)	A	B	C	D	E	F
Level 1	4.864	7.670	5.415	5.476	**6.016**	5.918
Level 2	**5.959**	5.851	5.008	5.121	4.793	5.221
Level 3	5.940	4.935	**5.961**	5.934	5.831	**5.936**
Level 4	5.399	4.787	5.615	5.219	5.517	5.388
Level 5	5.756	4.675	5.919	**6.168**	5.761	5.454
range	1.0953	2.9948	0.9525	1.0468	1.223	0.7144
rank	3	1	5	4	2	6

(E1) maximum compression speed 10 mm/s, and (F3) cooling time 5.6 s. The results presented in Fig. 5b confirm that these parameters settings yield a higher S/N ratio than any of the experimental runs in the Taguchi OA (including the standard conditions in Row #8).

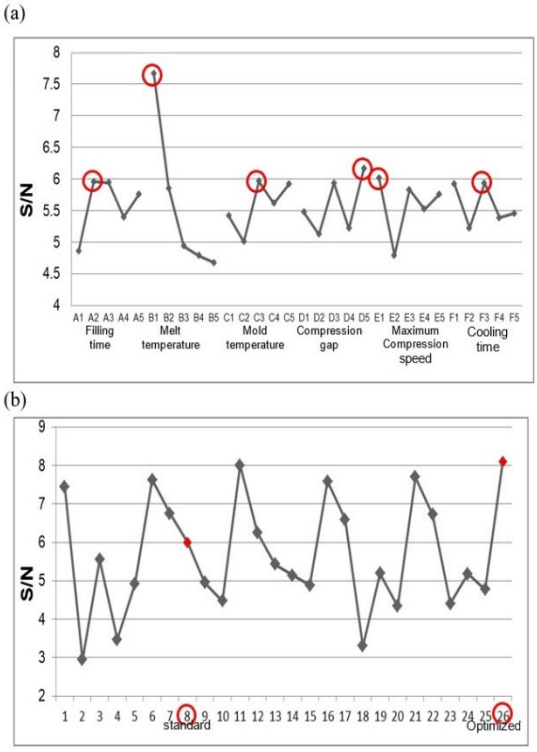

FIGURE 5. (a) Response diagram and (b) Confirmation results for optimization of OAD using method II.

B. TAGUCHI-GRA JOINT OPTIMIZATION OF OPD AND OAD (METHOD III)

Tables 6 and 7 present the S/N factor response results obtained from the Taguchi-GRA method for the joint optimization of the OPD and OAD quality characteristics. An inspection of Table 6 shows that the control factors can be ranked in terms of a diminishing impact on the two quality factors as follows: melt temperature > compression gap > filling time > maximum compression speed > cooling time > mold temperature. Moreover, the results presented in Fig. 6 indicate that the optimal processing conditions for jointly minimizing both the OPD and the OAD are as follows: (A3) filling time 1.8 s, (B5) melt temperature 250°C, (C3) mold temperature 60°C, (D5) compression gap 4 mm, (E1) maximum compression speed 10 mm/s, and (F1) cooling time 5.2 s.

C. TAGUCHI-GRA-FF METHOD JOINT OPTIMIZATION OF OPD AND OAD (METHOD IV)

The single-objective Taguchi analysis results presented in Section IV-A have shown that the melt temperature (Factor B) has the greatest effect on both the OPD and the OAD of the Fresnel lens. However, for the OPD, the optimal outcome is obtained using the highest melt temperature (250°C), while for the OAD, the optimal outcome is achieved using the lowest melt temperature (210°C). Accordingly, in implementing the fixed factor (FF) Taguchi experiments, the melt

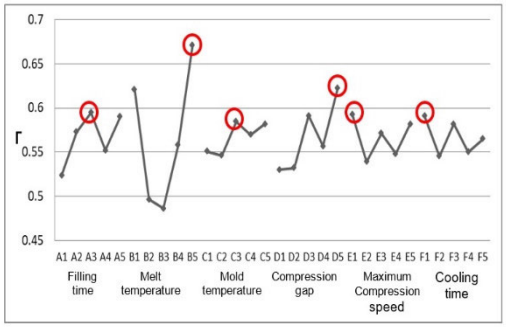

FIGURE 6. Taguchi S/N response diagram for joint optimization of OPD and OAD using Method III (Taguchi-GRA method).

TABLE 6. S/N response table for joint optimization of OPD and OAD using method III.

Γ	A	B	C	D	E	F
Level 1	0.524	0.621	0.551	0.530	0.593	0.591
Level 2	0.573	0.496	0.546	0.532	0.539	0.545
Level 3	0.595	0.486	0.585	0.591	0.571	0.582
Level 4	0.552	0.558	0.570	0.557	0.548	0.550
Level 5	0.590	0.671	0.582	0.622	0.582	0.565
range	0.071	0.185	0.039	0.093	0.053	0.045
rank	3	1	6	2	4	5

temperature was assigned the intermediate level setting of 230 °C, while the other control factors were varied in their original ranges (see Table 8). Table 9 shows the corresponding S/N response results obtained using the Taguchi-GRA-FF optimization method. It is seen that when the melt temperature is maintained at a constant value (fixed at 230°C), the OPD and OAD quality characteristics are determined mainly by the compression gap. Moreover, referring to Fig. 7, the optimal control factor level settings are found to be: (A5) filling time of 2.5 s, (B3) melt temperature of 230°C (Fixed), (C4) mold temperature of 65°C, (D5) compression gap of 4 mm, (E4) maximum compression speed of 17.5 mm/s, and (F3) cooling time of 5.6 s. For confirmation purposes, the Taguchi-GRA optimization method (Method III) was repeated using the optimal processing conditions determined in Section IV-B (i.e., A3C3D5E1F1), but with the melt temperature factor (Factor B) assigned control factor level settings of B1, B2, B3, B4 and B5 in turn. After normalization using the Max-Min method, the normalized S/N ratios were compared with the optimal values obtained using Methods I (OPD) and II (OAD), respectively. Table 10 shows the corresponding results. It is seen that of the five possible level settings for the melt temperature, only a temperature setting of 230°C yields a percentage difference of less than 50% from the optimal S/N value for both the OPD and the OAD. Hence, the optimal value of the melt temperature was confirmed to be 230°C. In other words, the optimal processing conditions were

TABLE 7. Taguchi-GRA results for S/N response for joint optimization of OPD and OAD using method III.

Trial NO.	OPD			OAD		
	x*	Δij	γ	x*	Δij	γ
1	0	1	0.333333	0.889091	0.110909	0.818453
2	0.134495	0.865505	0.366165	0	1	0.333333
3	0.507886	0.492114	0.503974	0.514163	0.485837	0.507183
4	0.650003	0.349997	0.588237	0.105119	0.894881	0.358453
5	0.987531	0.012469	0.975668	0.391495	0.608505	0.451058
6	0.08072	0.91928	0.352291	0.925542	0.074458	0.870386
7	0.339681	0.660319	0.430916	0.752984	0.247016	0.669329
8	0.597353	0.402647	0.553926	0.603661	0.396339	0.557825
9	0.677129	0.322871	0.607628	0.39735	0.60265	0.453453
10	0.884686	0.115314	0.812594	0.302488	0.697512	0.417532
11	0.105688	0.894312	0.3586	1	0	1
12	0.241421	0.758579	0.397274	0.653991	0.346009	0.59101
13	0.508663	0.491337	0.50437	0.492276	0.507724	0.496168
14	0.79441	0.20559	0.708627	0.434721	0.565279	0.469361
15	0.986173	0.013827	0.973091	0.382491	0.617509	0.447424
16	0.085045	0.914955	0.353368	0.917288	0.082712	0.858057
17	0.312015	0.687985	0.420881	0.720859	0.279141	0.641732
18	0.466203	0.533797	0.483654	0.070447	0.929553	0.34976
19	0.824657	0.175343	0.740365	0.445093	0.554907	0.473975
20	0.865673	0.134327	0.788236	0.274852	0.725148	0.408114
21	0.163659	0.836341	0.374156	0.939989	0.060011	0.892839
22	0.385227	0.614773	0.448522	0.747781	0.252219	0.6647
23	0.477563	0.522437	0.489027	0.289588	0.710412	0.413083
24	0.793071	0.206929	0.707285	0.441809	0.558191	0.472505
25	1	0	1	0.361829	0.638171	0.439301

determined to be (A5B3C4D5E4F3). For a final confirmation, the results obtained from Method IV for the optimal values of the OPD and OAD (A5B3C4D5E4F3) were compared with those obtained from Method III (A3B5C3D5E1F1, see Section IV-B). As shown in Table 11, given a melt temperature of 230°C (Method IV), the S/N value of the OPD is reduced by 4.34% compared to that obtained using Method III (i.e., −45.378 dB vs. −47.345 dB). However, that of the OAD is increased by 24.45% (4.888 dB vs. 6.083 dB). In other words, while Method IV achieves a slightly poorer optimization result for the OPD than Method III (an improvement of just 1.03% over the OPD achieved using the standard processing conditions compared to an improvement of 5.14% obtained by Method III), the optimization result obtained for the OAD is greatly improved (i.e., from −18.48% (Method III) to 1.45% (Method IV)).

D. PERFORMANCE COMPARISON OF FOUR OPTIMIZATION METHODS

As shown in Table 11, Method I (single-objective OPD Taguchi analysis method) improves the S/N ratio of the OPD characteristic by 5.77% compared to the solution obtained using the standard ICM processing conditions

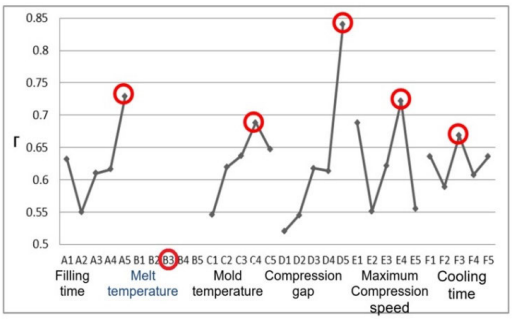

FIGURE 7. Taguchi S/N response diagram for joint optimization of OPD and OAD using Method IV (Taguchi-GRA-FF method).

TABLE 8. Factor level settings for fixed factor Taguchi experiments in Method IV.

Control factors	A (s)	B (°C)	C (°C)	D (mm)	E (mm/s)	F (s)
Level 1	1	230	50	2	10	5.2
Level 2	1.5	230	55	2.5	12.5	5.4
Level 3	1.8	230	60	3	15	5.6
Level 4	2	230	65	3.5	17.5	5.8
Level 5	2.5	230	70	4	20	6

TABLE 9. S/N response table for joint optimization of OPD and OAD using method IV.

Γ	A	B	C	D	E	F
Level 1	0.631	-	0.545	0.521	0.688	0.636
Level 2	0.550	-	0.619	0.545	0.551	0.589
Level 3	0.610	-	0.637	0.618	0.621	0.668
Level 4	0.616	-	0.688	0.613	0.721	0.607
Level 5	0.729	-	0.647	0.840	0.555	0.636
range	0.179	-	0.143	0.320	0.170	0.079
rank	2	-	4	1	3	5

TABLE 10. Evaluation of different melt temperature results in Method IV.

Temp. (°C)	OPD (dB)	Normal-ization	Δ%	OAD (dB)	Normal-ization	Δ%
210	-50.442	0.15425	-85%	7.8956	0.96	-4%
220	-49.109	0.36421	-64%	6.7312	0.7344	-27%
230	-47.345	0.64213	-36%	6.0829	0.6088	-39%
240	-46.61	0.75806	-24%	4.2479	0.2532	-75%
250	-45.218	0.97725	-2%	4.7590	0.3523	-65%

(A2B3C4D5E1F2). However, the S/N ratio of the OAD characteristic is reduced by −17.11 %. In other words, the improved OPD performance is obtained at the expense of the OAD. Consequently, in employing Method I, it is necessary to consider whether the improvement obtained in the birefringence of the molded lens outweighs the loss in imaging quality (i.e., aberrations) caused by geometric warpage. From the above analysis and discussion, if the only aim of the optimization process is to minimize the OPD (i.e., the birefringence effect) of the molded lens, then Method I (i.e., single-objective (OPD) Taguchi analysis) should be employed. For Method II (single-objective OAD Taguchi analysis method), the S/N value of the OPD is reduced by −6.11% compared to that obtained using the standard processing conditions. However, the S/N ratio of the OAD is increased by +35.12%. In other words, Method II provides a powerful approach for improving the OAD of the molded lens providing that a reduction in the OPD performance can be tolerated. From the above analysis and discussion, if the only goal of the optimization process is to minimize the OAD (i.e., the geometric distortion) of the molded lens, Method II (i.e., single-objective (OAD) Taguchi analysis) should be employed. For the multi-objective Taguchi-GRA optimization method (Method III), the S/N ratio for the OPD is 5.14% higher than that obtained using the standard operating conditions. However, the S/N ratio of the OAD is significantly lower (−18.48%). In other words, the multi-objective method reduces the birefringence of the molded lens, but increases the geometric warpage. The optimal solution for the OPD obtained using Method III is poorer than that obtained using the corresponding single-objective method (Method 1) (i.e., $+5.14\% < +5.77\%$). Moreover, the optimal solution for the OAD is also poorer than that of the solution obtained single-objective Method I (i.e., $-18.48\% < -17.11\%$). However, from a production perspective, Method III has a filling time of 1.8 s (A3), whereas Method I has a filling time of 2.5 s (A5). Thus, compared to Method I, Method III offers the opportunity to increase the production efficiency (and hence lower the cost) by reducing the cycle time. Furthermore, compared to the standard processing conditions, Method III provides the means to improve the OPD performance of the lens at the expense of a poorer OAD performance and slightly increased cycle time. Therefore, if the aim of the optimization process is to reduce the OPD of the molded lens and improve the production efficiency (i.e., reduce the cycle time), then Method III (multi-objective (OPD and OAD) Taguchi-GRA) should be employed provided that a poorer OAD performance can be tolerated.

For the Taguchi-GRA-FF optimization method (Method IV), the S/N values of the OPD and OAD are +1.03% and +1.45% higher than those obtained using the standard processing conditions, respectively. In other words, Method IV achieves a moderate improvement in both the birefringence and the aberration performance of the molded lens compared to that obtained using the standard operating parameters. However, this performance improvement is obtained at the expense of a longer cycle time (i.e., a filling time of 2.5 s in Method IV, but 1.5 s under the standard operating conditions). Finally, if the objective of the optimization approach is to reduce both the OPD and the OAD compared to that of the lens manufactured under the standard

TABLE 11. Performance evaluation of four optimization methods for OPD or/and OAD.

Method		Target	Factor Level	S/N (dB)			
				OPD	Δ%	OAD	Δ%
Standard			$A_2B_3C_4D_5E_1F_2$	-47.836	0.00%	5.996	0.00%
I	Taguchi	OPD	$A_5B_5C_5D_5E_1F_1$	-45.074	5.77%	4.970	-17.11%
II	Taguchi	OAD	$A_2B_1C_3D_5E_1F_3$	-50.761	-6.11%	8.102	35.12%
III	Taguchi GRA	OPD OAD	$A_3B_5C_3D_5E_1F_1$	-45.378	5.14%	4.888	-18.48%
IV	Taguchi GRA FF	OPD OAD	$A_5B_3C_4D_5E_4F_3$	-47.345	1.03%	6.083	1.45%

processing conditions, then Method IV should be employed. In this paper, only one factor is found to be significantly more influential than other factors after the Taguchi method analysis, so only one factor is fixed and its level is set at the middle value. However, if some processing conditions have more than two significant influence factors after the Taguchi method analysis, one can try to analyze the factors and levels according to the above method. However, if the number of significant influencing factors is too large or the analysis results are not good, it means that some factors are weak influencing factors, and these factors should be removed or the factors and levels of the Taguchi method (orthogonal array) should be redefined.

E. MELT TEMPERATURE EFFECT AND FLOW/THERMAL INDUCED STRESSES EFFECT

In general, the results presented in Table 11 show that the optimization results obtained for the OPD and OAD using Method III are poorer than those obtained using the corresponding single-objective Taguchi methods (i.e., Methods I and II, respectively). This can be attributed to a difference in the optimal melt temperature settings in the various methods. As discussed in Section IV-B, the melt temperature exerts a greater effect on the OPD and OAD than the other control factors and, in the case of the OPD particularly, dominates the S/N value. As a result, the level setting assigned to the melt temperature control factor greatly affects the results of all the experiments. As shown in Table 10, for any melt temperature setting other than the intermediate value of 230°C, either the OPD or the OAD is significantly degraded. Thus, in Method IV, the melt temperature is specifically chosen as 230°C. By selecting this particular value, the optimal OPD and OAD performances achieved at higher and lower melt temperatures of 250°C and 210°C, respectively, are deliberately sacrificed. However, this performance loss in one of the two quality metrics is judged to be outweighed by the moderate performance improvement obtained in both quality metrics compared to that that obtained under the standard operating conditions. Referring to Table 11, Method I (with optimal operating parameters of A5B5C5D5E1F1) yields the best OPD performance (S/N=-45.074 dB) of all the optimization methods. However, it achieves a poor OAD performance (S/N=4.970 dB). Similarly, Method II (with optimal operating parameters of A2B1C3D5E1F3) yields the best OAD performance of the four methods (S/N=8.102 dB), but the worst OPD performance (S/N=-50.761 dB). In other words, the results confirm that while both methods are capable of achieving a significant improvement in the target quality characteristic (i.e., OPD or OAD), they are inefficient when applied to the solution of multi-objective optimization problems. For the optimization problem considered in the present study, it is desirable to minimize the OPD of the molded lens in order to suppress the birefringence effect. Consequently, a higher melt temperature is beneficial since it reduces the melt viscosity during the compression stage, and therefore reduces the flow induced stress within the molded component. By contrast, to minimize the OAD of the molded lens, i.e., to minimize the geometric warpage of the lens, a lower melt temperature is desired in order to reduce the thermal induced stress produced during the cooling stage. Thus, referring to Table 12, the flow induced stress contribution toward the OPD is just 22.4% in Method II (in which the optimal temperature setting is determined to be 250°C (B5)). Similarly, in Method II (in which the optimal temperature setting is determined to be 210°C (B1)), the thermal induced stress contribution toward the OPD is only 35.6%. In other words, both methods successfully reduce the particular processing stress component associated with the corresponding quality characteristic (i.e., OPD and OAD, respectively). However, both methods fail to suppress the complementary stress component (i.e., the thermal induced stress component in Method I and flow induced stress component in Method II). Hence the limitations of both single-objective Taguchi methods in solving the present multi-objective optimization problem are again confirmed.

TABLE 12. Contributions of flow induced stress and thermal induced stress to OPD in methods I and II.

Method	Target	Average Value (nm)		
		OPD_{flow}	$OPD_{thermal}$	OPD
I	OPD	-8.482 (22.4%)	-29.318 (77.6%)	-37.8 (100%)
II	OAD	-43.484 (64.4%)	-24.077 (35.6%)	-67.561 (100%)

F. OPD, OAD AND FRINGE ORDER RESULTS OBTAINED UNDER DIFFERENT METHODS

Fig. 8 shows the simulation results obtained for the OPD, OAD and fringe patterns of the Fresnel lens produced using the standard ICM processing conditions and the processing conditions obtained using the four optimization methods, respectively. As shown, the OPD values of the five lenses vary in the range of 0 to 3800 nm, and are generally close to zero in most regions of the lens. However, the lens

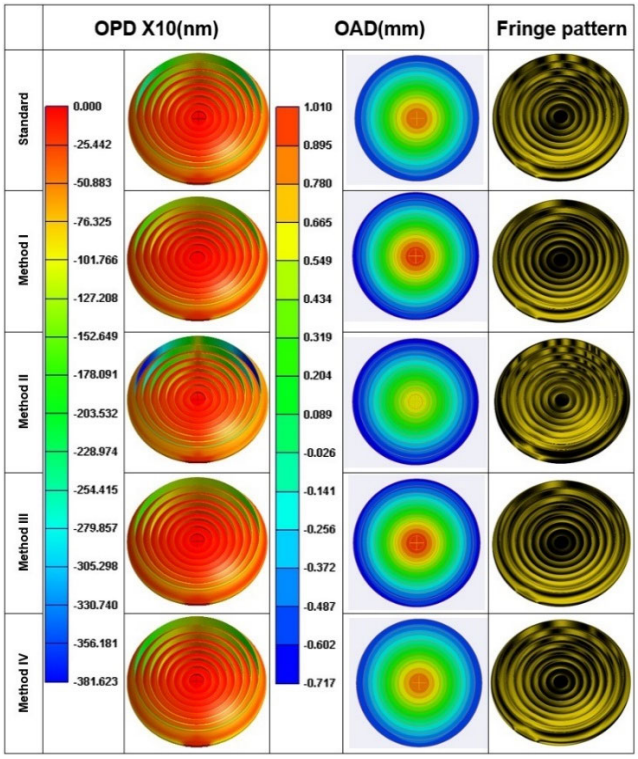

FIGURE 8. Simulation results for OPD, OAD and fringe patterns of lens produced using standard processing conditions and processing conditions obtained using methods I∼IV.

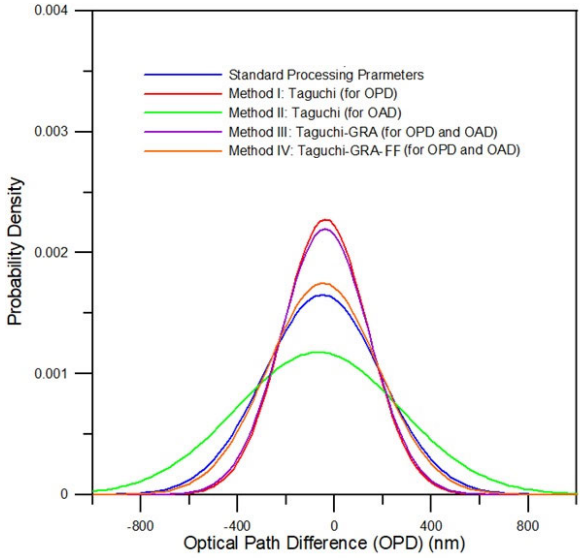

FIGURE 9. OPD improvement of methods I∼IV compared to standard process.

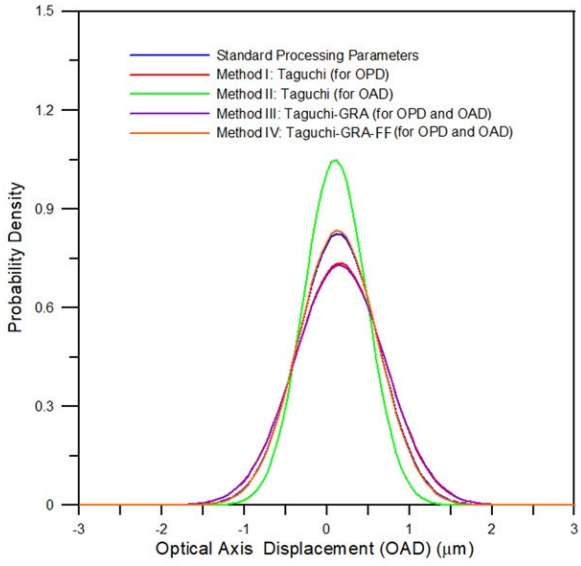

FIGURE 10. OAD improvement of Methods I∼IV compared to standard process.

fabricated using the molding conditions determined by Method II shows a region of significant retardation in the outer ring of the lens. All of the lenses show a negative displacement (i.e., a negative OAD value) in the outer ring, but a positive displacement in the central region. However, among all the optimization methods, Method II shows the least deformation of the lens in the central area. Overall, the results confirm that Methods I and II successfully reduce the OPD and OAD of the molded lens, respectively, while Method III improves the OPD in the central area of the lens, and Method IV yields a moderate improvement in both the OPD and the OAD. Table 13 shows the mean (μ) and standard deviation (σ) values of the OPD, OAD and fringe order of the Fresnel lenses produced using the standard ICM molding conditions and optimal molding conditions determined by the four optimization methods, respectively. The corresponding statistical distributions OPD and OAD by curve fitting with normal distribution are shown in Figs. 9 and 10, respectively. The results presented in Fig. 9 show that for all five methods, the OPD has a concentrated distribution about the center of the lens. Moreover, the results confirm that Method I yields an effective improvement in the OPD compared to the standard processing conditions. However, this performance improvement is obtained at the expense of the OAD (see Fig. 10). Hence, Method I is recommended only when the focus of the optimization process is to minimize the OPD of the lens. Similarly, Fig. 10 confirms that Method II improves the OAD performance of the molded lens, but at the expense of the OPD (see Fig. 9). Hence, Method II is recommended when the overriding aim of the optimization process is to minimize the OAD of the molded lens. Method III improves the OPD of the lens compared to that obtained using the standard processing parameters. However, the performance improvement is not as great as that achieved using Method I (see Fig. 9). Moreover, it yields the poorest OAD performance of the five methods. Thus, its use is not strongly recommended unless the aim of the optimization process is simply to improve the OPD performance of the lens compared to that of the original lens, while also reducing the injection cycle time compared to that of Method I).

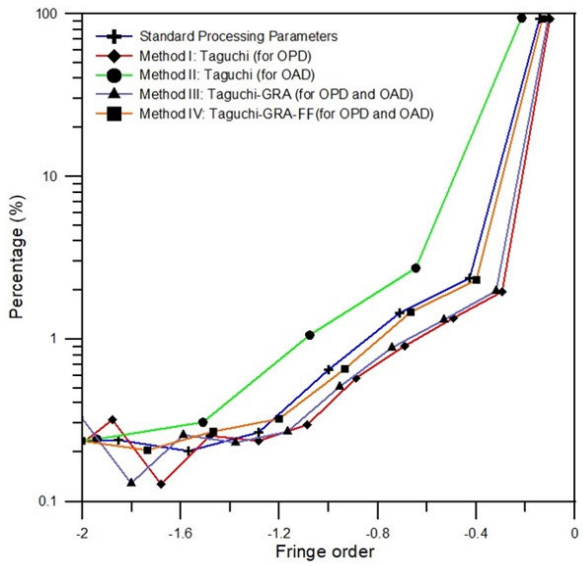

FIGURE 11. Fringe order improvement of Methods I∼IV compared to standard process.

TABLE 13. OPD, OAD and fringe order statistics for standard processing conditions and optimized processing conditions obtained using methods I∼IV.

Methods &Results	OPD (nm)		OAD (mm)		Fringe Order	
	μ	σ	μ	σ	μ	σ
Standard	-49.840	241.410	0.136	0.483	-0.084	0.409
Method I	-37.800	175.313	0.157	0.542	-0.064	0.297
Method II	-67.561	338.497	0.102	0.380	-0.115	0.574
Method III	-38.869	181.622	0.159	0.547	-0.066	0.308
Method IV	-47.281	228.106	0.134	0.478	-0.080	0.387

The results presented in Figs. 9 and 10 confirm that Method IV achieves a moderate improvement in both the OPD and the OAD of the lens. As such, Method IV is recommended when the objective of the optimization process is to improve both the OPD and the OAD performance of the lens. In general, the fringe order and OPD of an optical lens are strongly related. Thus, Method I achieves an effective improvement in the fringe order, as shown in Fig. 11. However, in optimizing the OAD performance of the molded lens, Method II degrades the OPD performance. As a result, the number of fringe orders increases significantly compared to the lens produced using the standard processing conditions.

V. CONCLUSION

This study combined Moldex3D flow simulation with four optimization methods (Methods I∼IV) to determine the processing conditions that minimize the OPD and OAD properties of plastic Fresnel lenses produced using the ICM process. The results show that the Taguchi method can effectively achieve specific results for the optimization of individual objectives. However, if more than two objectives are to be optimized for the manufacturing process, grey relational analysis is recommended. Finally, if the grey relational analysis method cannot get better results, it can be suggested to use the fixed factor method in this paper to solve the problem of two objective optimization and large difference in factor influence. Therefore, the suggestion to users is that each of the four optimization methods has advantages and disadvantages, and the choice of the method depends on the specific requirements of the optimization process.

REFERENCES

[1] O. Solorza-Nicolas, H. Hernandez-Moreno, O. Susarrey-Huerta, and N. Romero-Partida, "Film-insert injection compression molding for reinforced polycarbonate with woven glass fiber oriented 90/0°, ±45°" *Polym. Eng. Sci.*, vol. 59, no. 2, pp. 372–379, 2019.
[2] B. Fan, D. O. Kazmer, R. P. Theriault, and A. J. Poslinski, "Simulation of injection-compression molding for optical media," *Polym. Eng. Sci.*, vol. 43, no. 3, pp. 596–606, Mar. 2003.
[3] G. Ramorino, S. Agnelli, and M. Guindani, "Analysis of reactive injection compression molding by numerical simulations and experiments," *Adv. Polym. Technol.*, vol. 2020, pp. 1–8, Feb. 2020.
[4] H.-S. Lee and J.-R. Park, "Experimental study of injection-compression molding of film insert molded plates," *Int. J. Precis. Eng. Manuf.*, vol. 15, no. 3, pp. 455–461, Mar. 2014.
[5] N. H. Kim and A. I. Isayev, "Birefringence in injection-compression molding of amorphous polymers: Simulation and experiment," *Polym. Eng. Sci.*, vol. 53, no. 8, pp. 1786–1808, Aug. 2013.
[6] H. S. Lee and A. I. Isayev, "Numerical simulation of flow-induced birefringence: Comparison of injection and injection/compression molding," *Int. J. Precis. Eng. Manuf.*, vol. 8, no. 1, pp. 66–72, 2007.
[7] W. Cao, Z. Min, S. Zhang, T. Wang, J. Jiang, H. Li, Y. Wang, and C. Shen, "Numerical simulation for flow-induced stress in injection/compression molding," *Polym. Eng. Sci.*, vol. 56, no. 3, pp. 287–298, Mar. 2016.
[8] D. Loaldi, D. Quagliotti, M. Calaon, P. Parenti, M. Annoni, and G. Tosello, "Manufacturing signatures of injection molding and injection compression molding for micro-structured polymer Fresnel lens production," *Micromachines*, vol. 9, no. 12, p. 653, Dec. 2018.
[9] R. J. Crawford, *Plastics Engineering*. Oxford, U.K.: Pergamon, 1985.
[10] Y. Zhang, W. Yu, J. Liang, J. Lang, and D. Li, "Three-dimensional numerical simulation for plastic injection-compression molding," *Frontiers Mech. Eng.*, vol. 13, no. 1, pp. 74–84, Mar. 2018.
[11] C.-M. Lin and H.-K. Hsieh, "Processing optimization of Fresnel lenses manufacturing in the injection molding considering birefringence effect," *Microsyst. Technol.*, vol. 23, no. 12, pp. 5689–5695, Dec. 2017.
[12] C.-M. Lin and Y.-W. Chen, "Grey optimization of injection molding processing of plastic optical lens based on joint consideration of aberration and birefringence effects," *Microsyst. Technol.*, vol. 25, no. 2, pp. 621–631, Feb. 2019.
[13] S. Chatterjee, S. S. Mahapatra, and K. Abhishek, "Simulation and optimization of machining parameters in drilling of titanium alloys," *Simul. Model. Pract. Theory*, vol. 62, pp. 31–48, Mar. 2016.
[14] P. Zhao, W. Yang, X. Wang, J. Li, B. Yan, and J. Fu, "A novel method for predicting degrees of crystallinity in injection molding during packing stage," *Proc. Inst. Mech. Eng., B, J. Eng. Manuf.*, vol. 233, no. 1, pp. 204–214, Jan. 2019.
[15] N. Yeh and P. Yeh, "Analysis of point-focused, non-imaging Fresnel lenses' concentration profile and manufacture parameters," *Renew. Energy*, vol. 85, pp. 514–523, Jan. 2016.
[16] W. Wang, L. Aichmayer, B. Laumert, and T. Fransson, "Design and validation of a low-cost high-flux solar simulator using Fresnel lens concentrators," *Energy Proc.*, vol. 49, pp. 2221–2230, Jan. 2014.
[17] V. Kumar, R. L. Shrivastava, and S. P. Untawale, "Fresnel lens: A promising alternative of reflectors in concentrated solar power," *Renew. Sustain. Energy Rev.*, vol. 44, pp. 376–390, Apr. 2015.
[18] S.-C. Chen, Y.-C. Chen, H.-S. Peng, and L.-T. Huang, "Simulation of injection-compression molding process, Part 3: Effect of process conditions on part birefringence," *Adv. Polym. Technol.*, vol. 21, no. 3, pp. 177–187, 2002.

[19] C.-M. Lin and W.-C. Chen, "Optimization of injection-molding processing conditions for plastic double-convex Fresnel lens using grey-based Taguchi method," *Microsyst. Technol.*, vol. 26, no. 8, pp. 2575–2588, Aug. 2020.
[20] *Moldex3D Help 2022*. Accessed: Jun. 15, 2022. [Online]. Available: http://support.moldex3d.com/2022/en/index.html
[21] W. Michaeli and M. Wielpuetz, "Optimisation of the optical part quality of polymer glasses in the injection compression moulding process," *Macromol. Mater. Eng.*, vols. 284–285, no. 1, pp. 8–13, Dec. 2000.
[22] Y. Zhang, L. Li, T. Chen, and M. Song, "Optimization of Taguchi's on-line quality feedback control system," *Proc. Inst. Mech. Eng. B J. Eng. Manuf.*, vol. 231, no. 12, pp. 2173–2183, 2017.
[23] Y. Chen, A. Y. Yi, L. Su, F. Klocke, and G. Pongs, "Numerical simulation and experimental study of residual stresses in compression molding of precision glass optical components," *J. Manuf. Sci. Eng.*, vol. 130, no. 5, Oct. 2008, Art. no. 051012.
[24] A. Adhikari, T. Bourgade, and A. Asundi, "Residual stress measurement for injection molded components," *Theor. Appl. Mech. Lett.*, vol. 6, no. 4, pp. 152–156, Jul. 2016.
[25] J. M. Fischer, *Handbook of Molded Part Shrinkage and Warpage*, 2nd, ed. Amsterdam, The Netherlands: Elsevier, 2013.
[26] E. Dereniak and T. Dereniak, *Geometrical and Trigonometric Optics*. Cambridge, U.K.: Cambridge Univ. Press, 2008.
[27] F. Davì, "On the generalization of the Brewster law," *Math. Mech. Complex Syst.*, vol. 8, no. 1, pp. 29–46, May 2020.
[28] J. L. Rosa, A. Robin, M. B. Silva, C. A. Baldan, and M. P. Peres, "Electrodeposition of copper on titanium wires: Taguchi experimental design approach," *J. Mater. Process. Technol.*, vol. 209, no. 3, pp. 1181–1188, Feb. 2009.
[29] R. S. Rao, C. G. Kumar, R. S. Prakasham, and P. J. Hobbs, "The Taguchi methodology as a statistical tool for biotechnological applications: A critical appraisal," *Biotechnol. J.*, vol. 3, no. 4, pp. 510–523, Apr. 2008.
[30] R. S. Rao, R. S. Prakasham, K. K. Prasad, S. Rajesham, P. N. Sarma, and L. V. Rao, "Xylitol production by Candida sp.: Parameter optimization using Taguchi approach," *Process Biochem.*, vol. 39, no. 8, pp. 951–956, Apr. 2004.
[31] A. Ashrafi and K. Khalili, "Investigation on the effects of process parameters in pulsating hydroforming using Taguchi method," *Proc. Inst. Mech. Eng., B, J. Eng. Manuf.*, vol. 230, no. 7, pp. 1203–1212, Jul. 2016.
[32] D. Ju-Long, "Control problems of grey systems," *Syst. Control Lett.*, vol. 1, no. 5, pp. 288–294, 1982.
[33] K. H. Hsia and J. H. Wu, "A study on the data preprocessing in grey relation analysis," *J. Chin. Grey Syst.*, vol. 1, no. 1, pp. 47–54, 1998.
[34] M. K. Sahu, A. Valarmathi, S. Baskaran, V. Anandakrishnan, and R. K. Pandey, "Multi-objective optimization of upsetting parameters of Al–TiC metal matrix composites: A grey Taguchi approach," *Proc. Inst. Mech. Eng., B, J. Eng. Manuf.*, vol. 228, no. 11, pp. 1501–1507, Nov. 2014.
[35] J. Ren, J. Zhou, and J. Zeng, "Analysis and optimization of cutter geometric parameters for surface integrity in milling titanium alloy using a modified grey–Taguchi method," *Proc. Inst. Mech. Eng., B, J. Eng. Manuf.*, vol. 230, no. 11, pp. 2114–2128, Nov. 2016.
[36] S.-H. Chiu, S.-Y. Gan, Y.-C. Tseng, K.-T. Chen, C.-C. Chen, C.-H. Su, and S.-H. Pong, "Multi-objective optimization of process parameters in an area-forming rapid prototyping system using the Taguchi method and a grey relational analysis," *Proc. Inst. Mech. Eng., B, J. Eng. Manuf.*, vol. 231, no. 12, pp. 2211–2222, Oct. 2017.
[37] B. C. Jiang, S.-L. Tasi, and C.-C. Wang, "Machine vision-based gray relational theory applied to IC marking inspection," *IEEE Trans. Semicond. Manuf.*, vol. 15, no. 4, pp. 531–539, Nov. 2002.
[38] Q. Song and M. Shepperd, "Predicting software project effort: A grey relational analysis based method," *Expert Syst. Appl.*, vol. 38, no. 6, pp. 7302–7316, 2011.
[39] L. F. Wu, S. F. Liu, L. G. Yao, and S. L. Yan, "Grey convex relational degree and its application to evaluate regional economic sustainability," *Scientia Iranica*, vol. 20, no. 1, pp. 44–49, Dec. 2012.
[40] S. A. Javed, "A novel research on grey incidence analysis models and its application in project management," Ph. D. dissertation, Dept. Aeronaut. Astronauti., Nanjing Univ., Nanjing, P. R. China, 2019.

CHAO-MING LIN received the M.S. and Ph.D. degrees in mechanical engineering from the National Cheng Kung University, Taiwan, in 1993 and 1999, respectively. He is currently a Professor with the Department of Mechanical and Energy Engineering, National Chiayi University, Taiwan. He had some publications in the areas of electronic packaging, nanotechnology, microfluidics, and polymer processing, including more than 50 journal articles, more than 50 conference papers, more than 20 technical reports, and four patents. His research interests include IC packaging, injection molding processing, electrically conductive adhesive/films, nanotechnology, MEMS, and polymer packaging composites.

TING-HSUAN MIAU received the B.S. degree from the Department of Mechanical and Energy Engineering, National Chiayi University, Taiwan, in 2020. She is currently pursuing the master's degree with the Department of Mechanical Engineering, National Chung Kung University, Taiwan. Her research interests include MEMS and polymer processing.